GEOPHYSICAL RESEARCH LETTERS, VOL. 23, NO. 23, PAGES 3329-3332, NOVEMBER 15, 1996

Stratospheric temperature anomalies and mountain waves: A three-dimensional simulation using a multi-scale weather prediction model

Martin Leutbecher and Hans Volkert

DLR-Oberpfaffenhofen, Institut für Physik der Atmosphäre, Germany

Abstract. A non-hydrostatic weather prediction model with an interactive grid nesting facility (MM5) is used to infer the three-dimensional mesoscale temperature field over the Scandinavian mountains during 23 January 1991. Six hours after the initialization from operational analyses warm and cold anomalies of mesoscale extent developed on isentropic surfaces at stratospheric heights over the windward slope of the mountains and further downstream. Mean mesoscale temperature fluctuations along isentropes amount to more than 4 K while minima and maxima can differ by more than 30 K, consistent with height variations exceeding 3 km. Taking into account the three-dimensional motion field cooling rates up to 20 K/h are estimated.

Introduction

Polar stratospheric clouds (PSC) are important to stratospheric chemistry, especially the chemistry involved in polar ozone depletion. Crutzen and Arnold (1986) used this term for regions of enhanced background aerosol in the lower stratosphere and documented the high sensitivity of ozone to reactions involving nitrogen at low temperatures.

Stratospheric cloud observation in northern Europe were documented as early as 1870 (Stanford and Davis, 1974). Störmer (1929) made first precise height measurements by simultaneous photography from two locations separated by 27 km. A survey of his results obtained during four events is given in Figure 1. Due to their brilliant prismatic colours such clouds in the height interval of 20 to 30 km got the attribute *mother-of-pearl* or *nacreous*. The appearance of these clouds was related to significant cross-mountain flow with *Föhn-type* surface winds in the Oslo area.

Some *in-situ* measurements of stratospheric temperature fluctuations are available. Bacmeister et al. (1990; Figs. 1 and 2) found larger fluctuations of potential temperature (rms(θ')) up to 8 K) in areas above the Scandinavian mountains compared to flight legs over the ocean. Recently, Murphy and Gary (1995) evaluated the scale dependence of temperature fluctuations, which were obtained from aircraft measurements at altitudes of 9–14 km (airliners) and 18–21 km (microwave temperature profiler aboard ER-2). They distinguished four ranges spanning three decades in horizontal wavelength (15...15000 km) and showed that temperature variations are smaller for smaller wavelengths whereas the rate of temperature change increases with decreasing wavelength. They further argued that current operational weather prediction models were at best capable to capture fluctuations related to scales longer than 100 km, while the quasi-instantaneous rates of cooling and heating could not be reproduced according to the observations. At rare occasions stratospheric mountain waves were observed during research aircraft missions, e.g. by temperature and velocity sections at 19.7 km above southern Greenland (Chan et al., 1993) and upward looking Lidar profiles across the Scandinavian mountains (Godin et al., 1994).

Wave motions, which are induced by airflow over a mountain range, can propagate to stratospheric levels and instigate temperature anomalies relative to the synoptic scale atmospheric state. A calculation taylored to

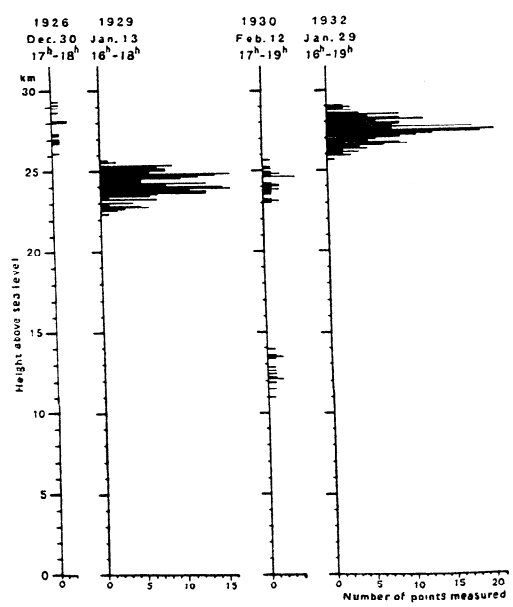

Figure 1. Height distribution of 516 photogrammetric measurements during 4 observing episodes of nacreous clouds over southern Norway. Adapted from Störmer (1940).

Paper number 96GL03240.
0094-8534/96/96GL-03240$05.00

the flow across the Scandinavian mountain range for 27 January 1992 but idealized to a non-rotating, two-dimensional section resulted in a temperature decrease of about 7 K in a region which air parcel trajectories passed in less than half an hour (Volkert and Intes, 1992). Such high resolution *temperature histories* serve as input for detailed microphysical PSC models (e.g. Peter et al., 1994).

Here a three-dimensional weather prediciton model is applied to infer the mesoscale temperature structures and their fluctuations, which are considered crucial for the formation of the various categories of PSC (see e.g. Toon et al., 1989). The earth's rotation is taken into account and, thus, the combination of flow over the mountains and around them is treated more realistically than in any two-dimensional simulation. First, the model set-up and initialization are outlined; the presentation of results for the 23 January 1991 case and their discussion make up the central part of the paper.

Model Set-up and Testing

The fifth generation Pennsylvania State University/ National Center for Atmospheric Research mesoscale model (MM5; Dudhia, 1993; Grell et al., 1994) is applied to one particular case of pronounced large scale flow across the Scandinavian mountains. The model integrates the fully compressible set of equations in a rotating frame of reference. In the nonhydrostatic version used here velocity (u, v, w), pressure perturbation p', and temperature T are prognostic variables.

Various horizontal scales can be effectively resolved within the computational domain due to a two-way mesh refinement scheme. Our case study hindcast of a situation with distinct cross mountain flow consists of a coarse domain with 36 km grid size (61×61 meshes; 2200 km domain length) and an imbedded nested area with 12 km spacing (82×82 meshes; 980 km subdomain length; see Fig. 2).

The model uses scaled reference pressure (σ) as vertical coordinate. The model top is set to 10 hPa ($\approx$ 28 km) where a radiative boundary condition absorbs vertically propagating gravity waves. The vertical resolution is about 0.5 km with a total of 53 levels. Terrain heights on both grids were obtained by interpolation from a 5′ orographic data set provided by the Geophysical Data Center (Boulder). Radiative and moist processes were switched off as the prime concern lies on the dynamics of mountain waves. The boundary layer is parameterized by the standard bulk formulation whereas turbulent mixing in the free atmosphere is taken into account by vertical diffusion which depends on the local Richardson number.

The initial conditions for 23 January 1991, 00 UTC and the boundary values during the integration over 24 h were derived from 12 hourly ECMWF analyses with a horizontal resolution of 2.5° in latitude and longitude and 15 levels between the surface and the 10 hPa pressure level. Over the integration period the synoptic scale fields of geopotential height and wind followed closely the development as it is documented in the *European Meteorological Bulletin* (DWD, Offenbach), both for the lower troposphere (700 hPa level) and just below the tropopause (300 hPa level). Therefore, we conclude that MM5 forced by ECMWF analyses is an apt framework for assessing the mesoscale response of three-dimensional cross mountain flow for selected cases.

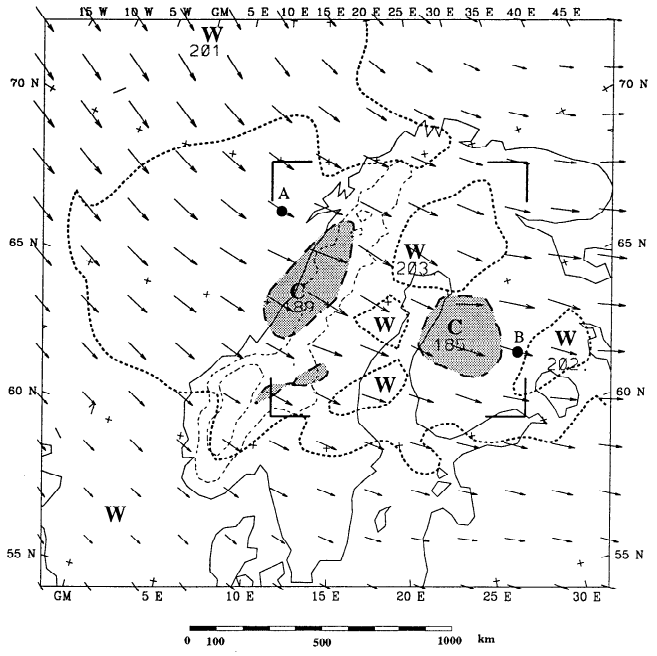

Figure 2. Flow and temperature structures at the potential temperature level $\theta = 440$ K (about 18.5 km high) for 23 Jan. 1991, 12 UTC after 12 h of simulation. The longest wind vector represents 65 m/s (air parcels travel an arrow length within 45 min). Isotherms (T = 199 K: bold dots; T = 194 K: bold dashes) bound warm (**W**) and cool (**C**; shaded) regions. The coastline (full) and the orography (500, 1000 m isohypses dashed) are indicated; the angles designate the nested region with threefold horizontal resolution ($\Delta x = 12$ km). **A** and **B** denote the end points of the cross-section in Figure 3.

Mesoscale Results for 23 January 1991

During the integration the wind veers from westerly to northwesterly directions exciting a transient gravity wave response. After the spin up time of about 6 hours large amplitude gravity waves are present in the stratosphere. Figure 2 shows the temperature and wind field on the isentropic surface $\theta = 440$ K at 12 UTC. This is within the period of maximum gravity wave activity in the lower stratosphere.

Higher isentropic surfaces overturn locally (Fig. 3). On time scales of less than a day the flow in the stratosphere is approximately adiabatic. An exception are the wavebreaking regions were considerable mixing occurs. Over a time of, say, 2 hours the wave pattern changes

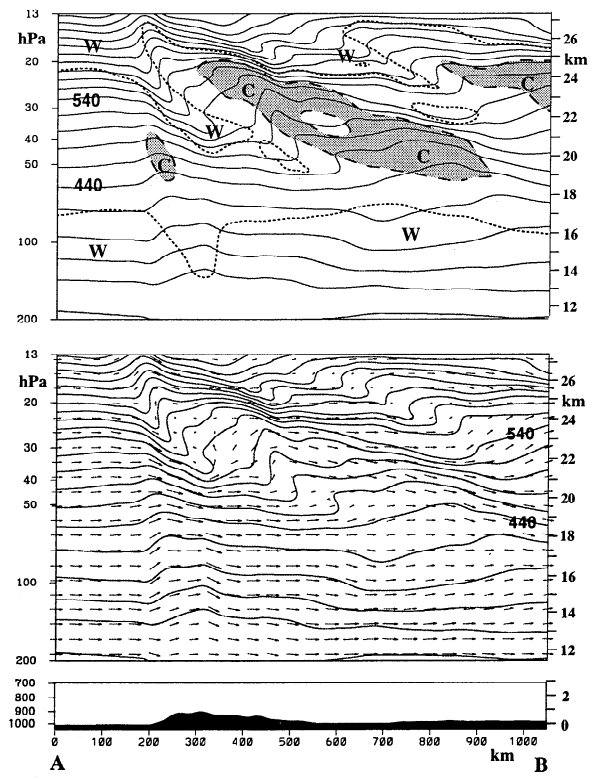

Figure 3. Cross-section through the nested area (see Fig. 2 for the positions **A** and **B**). Top: isentropes (contour interval: 20 K) and isotherms (T = 201 K, dotted; T = 191 K, dashed) bounding warmer regions (**W**) and colder ones (**C**; shaded). Middle: isentropes and flow within the section; the maximum speed is 69 m/s; air parcels travel an arrow length within 9 min. Bottom: model orography along the section.

little. Therefore one can estimate heating and cooling rates of up to 10 K/h on the $\theta = 440$ K level from Figure 2. At this level the temperature minimum of 185 K is located over Finland, some 15 K colder than in the upstream region.

At location **A** (see Figs. 2, 3) upstream of the orography temperatures are below 201 K in the height range 17 to 24 km with a minimum temperature of 194 K at 22.5 km. Due to the wave motions regions develop which are cooler or warmer with respect to the upstream conditions at location **A**. Figure 3 shows their vertical structure including an upstream tilt. Temperatures are higher (lower) compared to the upstream values where the isentropic surfaces are displaced downward (upward).

Horizontal temperature gradients amount to 10–20 K over 100 km in the hydraulic jump regions. Cooling rates of up to 20 K/h are estimated for these regions from Figure 3. The isentropes experience height variations of up to 3 km between their lowest and highest point. This results in temperature differences of more than 30 K along an isentropic surface (see Table).

Table. Mean temperature fluctuations $\sigma(T') = \mathrm{rms}(T-\overline{T})$ and maximal differences in temperature max ΔT and height max Δz within the layer 540 K $< \theta <$ 550 K every 4 h after model initialization. Data are taken from the nested area (cf. Fig. 2).

time	(h)	0	4	8	12	16	20	24
$\sigma(T')$	(K)	1.1	2.1	4.1	4.4	4.0	3.4	2.6
max ΔT	(K)	4	13	31	32	24	18	15
max Δz	(km)	1.2	1.9	3.2	3.5	2.6	2.0	1.7

Discussion

The simulation presented here shows that mountain flow induced temperature anomalies in the stratosphere can occur several hundred kilometers downstream of the mountain crest. For stationary, two-dimensional, and non-rotating flow the gravity wave activity is confined to the region above the mountain. For instance Volkert and Intes (1992) found in their simulations the cool regions directly above the mountain range. The rotation of the earth results in a leeward displacement of the longer wavelength gravity waves (Queney, 1948). Besides rotation the non-stationarity of the flow on the synoptic scale may account for gravity waves found at some distance from their source region (Lott and Teitelbaum, 1993).

At a height of 20–25 km where PSCs are typically observed we find large temperature fluctuations on isentropes. As gross quantitative information the Table lists as a function of simulation time: root mean square of temperature deviations at all gridpoints for a particular layer (540 K $< \theta <$ 550 K) and the difference between the maximum and the minimium in temperature (max ΔT) and height (max Δz). In the other layers ($\Delta\theta = 10$ K) between 500 and 600 K (height 20 to 25 km) the temperature fluctuations are of similar magnitude. Murphy and Gary (1995) estimated temperature fluctuations of 0.4–0.7 K for the wavelength range 63–628 km. In our nested region, where wavelengths from about 50–1000 km are resolved, fluctuations up to 4.4 K evolve during the integration. The aircraft data were averaged from many flights above land and sea where the average gravity wave activity is less pronounced than in a flow across a mountain range as discussed here. At the initial time ($t = 0$) the mean temperature fluctuation of the synoptic scale amounts to 1.1 K.

The maximum vertical displacement of isentropes exceeds 3 km during the period of strong wave activity (cf. Table and Fig. 3). Due to the breaking of the gravity waves larger amplitudes are not possible. The upstream values of windspeed ($\overline{U}$) and Brunt-Väisälä-frequency ($\overline{N}$) control the amplitude at which wave-breaking sets in. An estimate of the largest displacement possible is provided by considering the amplitude of a stationary sinusoidal gravity wave in a homogenous atmosphere. The vertical streamline displacement given by $\delta = a\sin(kx + mz)$ is a finite amplitude solution

of a stationary gravity wave if the dispersion relation $k^2+m^2 = \overline{N}^2/\overline{U}^2$ holds (Shutts et al., 1988). Assuming waves in the hydrostatic regime ($k \ll m$) yields a vertical wavenumber $m = \overline{N}/\overline{U}$. Convective instability prevents amplitudes larger than $a_s = \overline{U}/\overline{N}$, the saturation amplitude beyond which streamlines overturn. In the height range of 20 to 25 km the upstream values of wind speed and Brunt-Väisälä-frequency are approximately $\overline{U} = 35\,\mathrm{m/s}$, $\overline{N} = 0.024\,\mathrm{s}^{-1}$ giving a saturation amplitude of $2a_s = 2.9\,\mathrm{km}$. The maximum vertical displacement of isentropes is only slightly larger than this value (see Table). In the real atmosphere non-hydrostatic gravity waves with smaller vertical wavenumbers are also present. These could induce even larger vertical streamline displacements before wavebreaking sets in. Future work with increased horizontal resolution aims to also resolve this part of the wave spectrum.

The temperature variations along isentropes are related to the vertical displacement of the isentropes. For steady adiabatic flow of a perfect gas Bernoulli's theorem states that the sum $c_pT + gz + u^2/2$ of specific enthalpy, specific potential and kinetic energies is constant along a streamline, when friction and heat conduction can be neglected. If the speed is less than 50 m/s and the height of the streamline changes by more than 1 km, the potential energy change is one order of magnitude larger than the change of kinetic energy. For large amplitude waves one can therefore expect that the maximum temperature differences on a particular isentrope are approximately determined by the maximum height difference multiplied by the dry adiabatic lapse rate $\Gamma_d = g/c_p = 10\,\mathrm{K/km}$. The data from the numerical simulation show that this proportionality holds within 10% during the period of strong gravity wave activity.

In summary, we have demonstrated how a multi-scale weather prediction model can be applied to infer the dynamical input necessary for detailed microphysical modelling of PSC above complex terrain. The implementation of a three-dimensional trajectory package into the modelling system is underway as well as tests of the sensitivity to the height of the upper model boundary. High resolution raw data of radiosonde ascents ($\Delta t \approx 30\,\mathrm{s}$) are sought for a verification of the large amplitude waves.

The mean temperature fluctuations on horizontal scales of 50 to 1000 km are calculated to be about 5 times larger in our case of cross-ridge flow than those estimated from aircraft measurements over the oceans and mostly flat terrain, consistent with results from the AASE campaign (Bacmeister et al., 1990). A systematic stratospheric probing of orographically perturbed flows remains to be undertaken.

Acknowledgments. The authors thank Georg Grell (IfU, Garmisch) for his advice concerning the MM5 modelling system and Bill Kuo (NCAR, Boulder) for the permission to use it.

References

Bacmeister, J.T., M.R. Schoeberl, L.R. Lait, P.A. Newman, B. Gray, Small-scale waves encountered during AASE, *Geophys. Res. Lett., 17,* 349-352, 1990.

Chan, K.R., L. Pfister, T.P. Bui, S.W. Bowen, J. Dean-Day, B.L. Gary, D.W. Fahey, K.K. Kelly, C.R. Webster and R.D. May, A case study of the mountain lee wave event of January 6, 1992, *Geophys. Res. Lett., 20,* 2551-2554, 1993.

Crutzen, P.J. and F. Arnold, Nitric acid cloud formation in the cold Antarctic stratosphere: a major cause for the springtime 'ozone hole', *Nature, 324,* 651-655, 1986.

Dudhia, J., A non-hydrostatic version of the Penn State–NCAR Mesoscale Model: Validation tests and simulation of an Atlantic cyclone and cold front, *Mon. Weather Rev., 121,* 1493-1513, 1993.

Godin, S., G. Mégie, C. David, D. Haner, C. Flesia, and Y. Emery, Airbourne lidar observation of mountain-wave-induced polar stratospheric clouds during EASOE, *Geophys. Res. Lett., 21,* 1335-1338, 1994.

Grell, G.A., J. Dudhia, and D.R. Stauffer, A description of the fifth-generation Penn State/NCAR mesoscale model (MM5), *Techn. Note 398,* 121 pp., National Center for Atmospheric Research, Boulder, CO, 1994.

Lott, F. and H. Teitelbaum, Linear unsteady mountain waves, *Tellus, 45A,* 201-220, 1993.

Murphy, D.M. and B.L. Gary, Mesoscale temperature fluctuations and polar stratospheric clouds, *J. Atmos. Sci., 52,* 1753-1760, 1995.

Peter, T., R. Müller, P.J. Crutzen and T. Deshler, The lifetime of leewave-induced ice particles in the Arctic stratosphere: II. Stabilization due to NAT-coating, *Geophys. Res. Lett., 21,* 1331-1334, 1994.

Queney, P., The problem of air flow over mountains: A summary of theoretical studies, *Bull. Am. Meteorol. Soc., 29,* 16-26, 1948.

Shutts, G.J., M. Kitchen and P.H. Hoare, A large amplitude gravity wave in the lower stratosphere detected by radiosonde, *Q. J. R. Meteorol. Soc., 114,* 579-594, 1988.

Stanford, J.L. and J.S. Davis, A century of stratospheric cloud reports: 1870-1972, *Bull. Am. Meteorol. Soc., 55,* 213-219, 1974.

Störmer, C., Remarkable clouds at high altitudes, *Nature, 123,* 260-261, 1929.

Störmer, C., Höhenbestimmung von Perlmutterwolken von 1926 bis 1934, *Beitr. Phys. fr. Atmos., 26,* 119-120, 1940.

Toon, O.B., R.P. Turco, J. Jordan, J. Goodman and G. Ferry, Physical processes in polar stratospheric ice clouds, *J. Geophys. Res., 94,* 11359-11380, 1989.

Volkert, H. and D. Intes, Orographically forced stratospheric waves over Scandinavia, *Geophys. Res. Lett., 19,* 1205-1208, 1992.

M. Leutbecher and H. Volkert, DLR-Oberpfaffenhofen, Institut für Physik der Atmosphäre, D-82230 Weßling, Germany. (e-mail: Martin.Leutbecher@dlr.de; Hans.Volkert@dlr.de)

(received July 18, 1996; revised September 25, 1996; accepted September 25, 1996.)